# Method for forecasting the flood risk in a tropical country

Adriana Marquez, Bettys Farias and Edilberto Guevara


## ABSTRACT

In this study, a novel method for forecasting the flood risk in a tropical country is proposed, called CIHAM-UC-FFR. The method is based on the rainfall–runoff process. The CIHAM-UC-FFR method consists of three stages: (1) calibration and validation for the effective precipitation model, called CIHAM-UC-EP model, (2) calibration of forecasting models for components of the CIHAM-UC-EP model, (3) proposed model for forecasting of gridded flood risk called CIHAM-UC-FR. The CIHAM-UC-EP model has a mathematical structure derived from a conceptual model obtained by applying the principle of mass conservation combined with the adapted principle of Fick's law. The CIHAM-UC-FR model is a stochastic equation based on the exceedance probability of the forecast effective precipitation. Various scenarios are shown for a future time where the flood risk is progressively decreased as the expected life parameter of the hydraulic structure is increased.


**Key words** | effective precipitation, effective precipitation forecasting model, flow attenuation, flow attenuation time, forecasting model, gridded forecast flood risk

**Adriana Marquez** (corresponding author)
**Bettys Farias**
**Edilberto Guevara**
Center of Hydrological and Environmental Research,
University of Carabobo,
Naguanagua,
Venezuela
E-mail: *ammarquez@uc.edu.ve*

## HIGHLIGHTS

- Flood risk forecasting method.
- Flood risk forecasting model (CIHAM-UC-FFR).
- Effective precipitation forecasting model.
- Effective precipitation model calibration and validation (CIHAM-UC-EP).
- Two-dimensional modeling of flood risk.

## INTRODUCTION

The definition of flood risk is a concept adapted to multiple and different empirically estimated variables. The definition of flood risk (FR) has evolved from the beginning of the 21st century to the present. The FR was a diffuse variable inferred indirectly through hazard and vulnerability maps. From the second decade of the 21st century, the flood risk was weighted by combining the hazard and vulnerability variables, which were represented on the map (Farias *et al.* 2020a).

The flood hazard is determined by the variables that cause flooding. Two main causes or mechanisms are attributed to flooding events, atmospheric and geotechnical (Sene 2008). The atmospheric mechanisms comprise frontal depressions, thunderstorms, monsoon, tropical cyclones (hurricanes and storms), snowmelts, and ice jams. The geotechnical mechanisms include tsunamis and debris flow.

The variables associated with these mechanisms and linked to the flood hazard are depth, velocity, extent and debris. The vulnerability to flooding is characterized by the location and number of people likewise, the properties under risk, whose variables constitute the basis for the community-level plans, and organizational structures (Farias *et al.* 2020a).

Until the present, the focus for forecasting has been the flood event. The flood forecasting models are based on observations of river levels and rainfall higher in a catchment (for river flooding), or of tidal levels, wave heights, wind speed and other parameters (for coastal flooding) (Schumann 2011).

doi: 10.2166/ws.2020.129

Process-based methods for modeling river levels, flows and velocities, on the floodplain can include (Sene 2008): one-dimensional models for the main river channel, with projection of levels onto the floodplain, or separate pathways for main channel and floodplain flows; one-dimensional models including floodplain pathways represented via spill units, compartments and/or cells; two-dimensional models of the floodplain using digital terrain models based on mass conservation, or including momentum effects; fully two- or three-dimensional models of the floodplain incorporating features on the floodplain such as buildings, embankments, and gulleys among others, and possibly urban drainage networks.

In recent studies, Farias *et al.* (2020b) developed a method for estimating flood risk, supported by the physical process of rainfall–runoff determined by applying the US Soil Conservation Service (US-SCS) to obtain the effective precipitation (EP). The US-SCS-EP is linked to the exceedance probability used as an input factor to the equation for the water-control design due to the occurrence of extreme hydrological events (Chow *et al.* 1988; Guevara & Cartaya 2004; Farias *et al.* 2020a). The US-SCS-EP is estimated based on water balance in the soil surface adjusted by a correction factor considering the previously stored water in the soil matrix. The US-SCS-EP method tends to produce homogeneous values due to the exclusion of the effects of variation in terrain elevation, slope and relief.

In this study, a novel method of forecasting flood risk is proposed, called CIHAM-UC-FFR. The method is based on the rainfall–runoff process. The CIHAM-UC-FFR method consists of three stages: (1) calibration and validation for the effective precipitation model, named the CIHAM-UC-EP model, (2) calibration of forecasting models for components of the CIHAM-UC-EP model, (3) proposed model for forecasting of gridded flood risk, named CIHAM-UC-FR. The CIHAM-UC-EP model has a mathematical structure derived from a conceptual model obtained by applying the principle of mass conservation combined with the principle of Fick's law. The CIHAM-UC-FR model is a stochastic equation based on the exceedance probability of the forecast effective precipitation.

The main difference of the proposed method when comparing with the historical flood risk definition is the relationship with a variable, such as the effective precipitation, that represents the flow on the watershed surface, considering its use and coverage such as urban, agricultural, rangeland, vegetation, water bodies, and degraded soil, among others. In the preceding definitions, the flood risk is indirectly associated with the hydrological variables through the flooding hazard. Moreover, the hydrological variables are connected, in a restricted way, to the flooding caused by a river in its adjacent areas. In the proposed method, the river is part of the elements that cause flooding, however it can be generated by surface flow on the ground in paved areas (urban) or on impervious soil.

In CIHAM-UC-EP, effective precipitation is estimated by combining the principle of conservation of masses together with a first-order law established by Fick to explain the temporal dynamics of the rate of substance consumption associated with the dissipation gradient of the concentration of substances as their molecules move in a predominant direction within an aqueous medium. In the proposed equation, this principle is applied to explain the dynamics of the rate of attenuation of water depth following a specific flow path by estimating an attenuation coefficient that represents the spatio-temporal dynamics. The attenuation coefficient implies loss by infiltration, bed roughness, and evaporation. Furthermore, the proposed equation incorporates as an input variable the downstream flow length (Olivera *et al.* 1998) calculating distance along a flow path considering the elevation changes of the ground. These dynamic elements to estimate the effective precipitation constitute a notable difference with respect to the method proposed in studies such as Farias *et al.* (2020a).

With respect to the forecasting model, the previous discussion can be extended to this aspect, due to the traditional variable the flooding is expressed in terms of flow-depth, flow-velocity or flow-extent. In that sense, in this study, the forecast is on the flood risk variable defined by the exceedance probability of effective precipitation being modified by a parameter depending on the expected life of the hydraulic structures that could be proposed as a water-control measure.

## THEORETICAL FORMULATION

In this study, the theoretical formulation for forecasting of flood risk in a tropical basin comprises as a main process the rainfall–runoff renamed as effective precipitation,

which is estimated based on a spatially distributed conceptual model. The forecast effective precipitation is obtained from time series models. Subsequently, flood risk forecasting is supported by the exceedance probability of forecast effective precipitation in the study area.

## Conceptual model for estimating of effective precipitation

### Equation for water mass balance in the open channel

The effective precipitation modeling is framed into the commonly used models of rainfall–runoff process (Márquez & Guevara 2013). The formulation of the model is developed by combining the fundamental equations that explain the motion of fluids and the advection–diffusion process for mass transport supported by the principle of mass conservation applied to an open channel.

The equation of mass conservation is derived from a control volume where the water flows along the natural open channels, with a flow area of variable cross-section $A$ ($dydz$), which is taken perpendicularly to the flow velocity vector assumed as the direction $x$ (Szymkiewicz 2010). The mass balance for the volume element is expressed by Equation (1):

$$\frac{\partial \rho}{\partial t} dxdydx = (\rho u dydz + \rho q_s dx) - \left[\rho u + \frac{\partial}{\partial x}(\rho u)dx\right] dydz \quad (1)$$

where the temporal variation of mass is represented as $(\partial\rho/\partial t)\, dxdydx$ and $\rho$ is the water density. The input flow in the element in the direction $x$ is $(\rho u dydz + \rho q dx)$, with $u$ being the velocity in the direction $x$, $\rho q_s dx$ the lateral inflow of mass, and $q_s$ the lateral inflow. The output flow from the element through the limit downstream in the direction $x$ is $[\rho u + (\partial/\partial x)(\rho u)dx]dydz$, with $(\partial/\partial x)(\rho u)dx$ being the change in the discharge on $x$. Equation (1) can be expressed as follows:

$$(\rho u A + \rho q dx) - \left[\rho u A + \frac{\partial}{\partial x}(uA)dx\right] = \rho \frac{\partial A}{\partial x} dx \quad (2)$$

Assuming the approximation to a prismatic channel with a rectangular shape of width $W$ and depth of flow $h$, $[h = h(x, t)]$, Equation (2) can be expressed as follows:

$$W \frac{\partial h}{\partial t} + W \frac{\partial (uh)}{\partial x} - q_s = 0 \quad (3)$$

$$\frac{\partial h}{\partial t} + u \frac{\partial h}{dx} + h \frac{\partial u}{\partial x} - \frac{q_s}{W} = 0 \quad (4)$$

In the case of non-lateral inflow and one-dimensional flow, assuming that in the stream the only velocity occurs in favor of the stream $u$, in the direction $x$, Equation (4) can be reduced as follows:

$$\frac{\partial h}{\partial t} = -\frac{\partial (uh)}{\partial x} \quad (5)$$

### Equation for unsteady flow in open channel

In this study, one of the novelties consists of proposing a mathematical expression for explaining the unstable flow due to the attenuation of the flow depth provided by an external source as the precipitation associated with the term $uh$ (Equation (5)) (Márquez & Guevara 2013). This term is an approximate expression for the discharge entering an open channel of unit width being decreased in a proportion specified by an attenuation coefficient $A_f$ that influences the flow depth consumption rate along the channel in the downstream direction $x$ ($\partial h/\partial x$).

The decreasing of flow depth transported along the drainage channel could be explained by different bed roughness depending on the degree of vegetal coverage, different bed elevations influencing the variation of the longitudinal bottom slope, and soil type, and likewise physical processes such as infiltration and evaporation, among others. Equation (6) has been demonstrated for explaining the mass transport that moves from an area of higher concentration to another of lower concentration in a prevalent flow direction, known as Fick's Law for the molecular diffusion process of chemical species (Guevara 2016):

$$uh = -A_f \frac{\partial h}{\partial x} \quad (6)$$

Substituting in Equation (5), it is obtained that:

$$\frac{\partial h}{\partial t} = -A_f \frac{\partial^2 h}{\partial x^2} \tag{7}$$

The analytical solution of the model for unsteady flow depth in an open channel is shown in Equation (8). The flow depth is attenuated to the downstream direction in the output of the drainage channel ($h_o$), named also as the effective precipitation (EP), caused by the water sheet that enters the drainage channel due to the occurrence of precipitation, represented as the total flow depth in the input to the drainage channel in the upstream direction ($h_i$) (Márquez & Guevara 2013). A variable that takes into account a grid of land use and land cover (LULC) factor has been added, which is represented by the curve number (CN) (Soil Conservation Service 1986). The parameters are $a$ and $t$, $a$ representing the attenuation coefficient of flow depth along the channel and $t$ an approach to the time for attenuation of the flow depth associated with the precipitation event. These terms are related as indicated in Equation (8):

$$(h)_o(x, t) = \frac{CN(h)_i}{\sqrt{4\pi a t}} \exp^{((-x^2)/(4at))} \tag{8}$$

where $x$ is the flow length in the downstream direction. In the conceptual model for effective precipitation (EP) proposed by CIHAM-UC (CIHAM-UC-EP), both variables and parameters are measured (Feldman 2000); $t$ might be approximated to the concentration time $t_c$ estimated as an approximation to the travel time in the channel ($t_{channel}$), for non-lateral inflow. $A_f$ is the infiltration rate measured in field studies expressed in m/h by flow length (m) and unit width of drainage channel (m) (Guevara & Marquez 2012; Márquez & Guevara 2011b; Márquez 2009).

## Models for spatial distribution prediction of precipitation

The models of precipitation spatial distribution prediction are applied, using the values of the target variable ($z$) at some location $s_0$. The predictions are based on the model (Márquez *et al.* 2019):

$$Z(s) = \mu + \varepsilon'(s) \tag{9}$$

where $\mu$ is the constant stationary function (global mean) and $\varepsilon'(s)$ is the spatially correlated stochastic part of variation.

## Lumped time-series models for forecasting of the components of the equation for unsteady flow in open channel

Lumped models are proposed for forecasting of the components of the equation for unsteady flow in an open channel (CIHAM-UC-EP). The components involved are the precipitation and the parameters $A_f$ and $t$. ARIMA (AutoRegressive, Integrated, Moving Average) models (Box & Jenkins 1970) are used to evaluate the adjustment of the time series of components (Márquez & Guevara 2016).

## Lumped models for probabilistic distribution of effective precipitation

The probabilistic functions that have been tested for adjusting to hydrological variables are the following (Guevara & Cartaya 2004): normal, exponential, extreme values, Weilbull, among others.

## Empirical model for estimating the flood risk

The flood risk is determined using the modified equation for water-control design due to the occurrence of extreme hydrological events (Guevara & Cartaya 2004) indicated in Equation (10) and adapted to predict the flood risk (Chow *et al.* 1988; Farias *et al.* 2020a):

$$R = 1 - [1 - p(X \geq x_T)]^n \tag{10}$$

where $R$ represents the probability that an event $X \geq x_T$ will occur at least once in $n$ years, $T$ being the design return period, $p(X \geq x_T) = 1/T$ is the exceedance probability of the effective precipitation, and $n$ is the expected life of the hydraulic structure as a control measure for flooding.

In this study, a modification of Equation (10) is proposed for forecasting of flood risk (FR), named CIHAM-UC-FR, as follows:

$$FR = [1 - p(X \geq x)]^n \quad (11)$$

where $FR$ is the flood risk, and $p(X \geq x)$ is the exceedance probability derived from a probabilistic distribution function fitted to the effective precipitation.

## METHOD

The proposed method to forecast spatial distribution of flood risk in a basin is developed in three stages: (1) calibration and validation of the effective precipitation model, (2) calibration of forecast models for components of the EP-CIHAM UC model and (3) the proposed model for forecasting of gridded flood risk (CIHAM-UC-FR).

### Calibration and validation of effective precipitation model

#### Data for calibration of effective precipitation model

The proposed model of effective precipitation (Equation (8)) is calibrated using four types of data: (a) time series of maximum precipitation for a duration of six hours for the period 1980–2018, (b) satellite images for the period 1979–2018, (c) map of soil types, (d) digital elevation model.

*Time series of maximum precipitation for a duration of six hours*: time series of precipitation were collected from three sources during three periods (Figure 1):

(a) *Hydrology and Meteorology Directorate (HMD) – Ministry of Environment and Natural Resources (MENR)* collected precipitation data through an automatic hydrometeorological observation network at national scale during the period 1980–2000, using weighing–recording gauges with a strip-chart data logger. The MENR-HMD yielded records of maximum precipitation ($P_{max}$) for durations of 1 h, 3 h, 6 h, 12 h, 9 h and 24 h. In this study, the $P_{max}$ time series from 48 gauges located in eight states is used (Figure 1) (Márquez *et al.* 2018; Farias *et al.* 2020b).

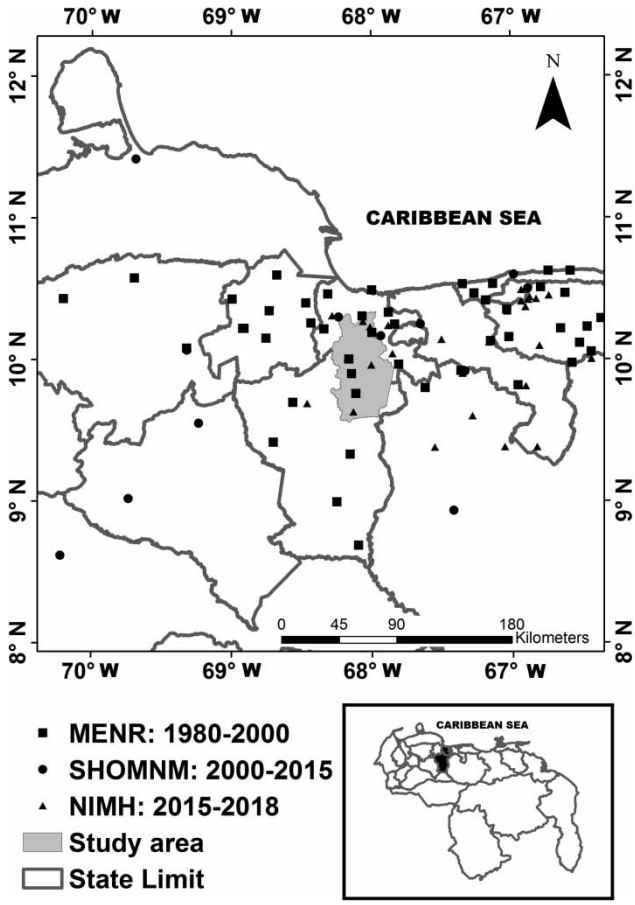


**Figure 1** | Location of meteorological stations corresponding to three sources of data collection grouped by periods: (1) 1980–2000: Ministry of Environment and Natural Resources – Hydrology and Meteorology Directorate (MENR-HMD), (2) 2000–2015: Service of Hydrology, Oceanography, Meteorology and Nautical Mapping (SHOMNM) – Bolivarian Army (BM) – Ministry for Defense (MD), (3) 2015–2018: National Institute of Meteorology and Hydrology (NIMH) – Ministry of Internal Relations, Justice and Peace (MIRJP).

(b) *Service of Hydrology, Oceanography, Meteorology and Nautical Mapping (SHOMNM) – Bolivarian Army (BM) – Ministry for Defense (MD)* generated $P_{max}$ records applying the method of MENR-HMD for airports of Venezuela, and the $P_{max}$ data are extracted from eleven gauges (Figure 1) (Infante *et al.* 2008).

(c) *National Institute of Meteorology and Hydrology (NIMH) – Ministry of Internal Relations, Justice and Peace (MIRJP)* collected precipitation data by a telemetering automatic hydrometeorological observation network at national scale during the period 2015–2018, using tipping-bucket rain gauges with a telecommunication platform consisting of Ultra-High Frequency (UHF)

and Extreme High Frequency (EHF) transmitters (Meza 2007). The records for precipitation measured each five minutes were obtained from 18 rain gauges (Figure 1) (Márquez *et al.* 2018; Farias *et al.* 2020b).

*Satellite images*: 20 Landsat images were acquired for the period 1979–2018, corresponding to a single scene, where the Pao River basin is contained. The temporal series of images from the four Landsat satellites were grouped according to the type of Landsat satellite (Márquez *et al.* 2019): (1) L2 MSS (1979), (2) L4TM (1987, 1988, and 1989), (2) L5TM (1984, 1986, 1990, 1991, 1996, 1997, 1998, 1999, 2000 and 2001), (3) L7ETM (2002 and 2003) and (4) L8OLI (2014, 2015, 2016, 2017, and 2018).

*Raster map of soil type* for the study unit was obtained by vectorization and subsequent rasterization processes from the source map made for Venezuela, setting the cell size to 30 m (Farias *et al.* 2020a).

*Digital elevation model (DEM)*: four ASTER (Advance Spaceborne Thermal Emission and Reflection Radiometer) Global DEMs covering the study area, the Pao River basin, were acquired from the Earthexplorer website, identified as ASTGDEMV2_0N09W068, ASTGDEMV2_0N09W069, ASTGDEMV2_0N10W068, ASTGDEMV2_0N10W069.

## Variables for the calibration of the effective precipitation model

The data were acquired and estimated applying three methods that allow the spatial distribution to be obtained (Figure 2): (a) maximum precipitation, (b) land use and land cover factor, and (c) flow length.

*Raster map of maximum precipitation* (Figure 2): the monthly spatial maximum precipitation for a duration of 6 h prediction was obtained applying Equation (10) constituted by two terms. The first term, the global mean of precipitation, was calculated based on the number of rain gauges within the study area (Figure 1). The second term is the spatially correlated stochastic part of the variation predicted using an experimental variogram fitted to a *J*-Bessel function (Márquez *et al.* 2019). A total of 456 monthly maximum rainfall raster maps were estimated for a duration of 6 h in the study area (Figure 3(a)), the cell size being 500 m.

*Raster map of land use and land cover factor* (Figure 2): the raster map of land use and land cover (LULC) factor is defined as the curve number (CN) (Soil Conservation Service 1986), which is obtained by superimposing the soil type and land use and land cover (LULC) raster maps. The soils of the Pao River basin have predominantly particles from fine and finest, being classified as class C (moderately high runoff) and D (high runoff) according to the hydrologic classification system of US-SCS. The land cover/land use raster maps in the study area were estimated using the Landsat satellites finding the following results (Farias *et al.* 2018; Márquez *et al.* 2018, 2019; Farias *et al.* 2020b): (1) urban (5%), (2) agricultural (0.6%), (3) rangeland (26%), (4) vegetation (40.5%), (5) degraded soil (24.4%) and (6) water bodies (1.5%).

*Raster map of downstream flow length* (Figure 2): the hydrologically corrected terrain data (DEM) were used with a cell size of 30 m as input (Fleming & Doan 2013). The flow length was derived in Geographical Information System (GIS). The downstream flow length to the watershed outlet was calculated as the difference between the flow length value of the cell and the flow length value of its corresponding outlet cell (Olivera *et al.* 1998).

## Calibration of CIHAM-UC effective precipitation model (Figures 2 and 3)

The calibration of the CIHAM-UC effective precipitation (CIHAM-UC-EP) model was made using statistical software to solve the non-linear equation by applying a *steepest descent* algorithm for the fitting of the parameters. The 456 mean values of the two fitted parameters, $A_f$ and $t$, are represented in Figure 3(b) and 3(c).

## Validation of CIHAM-UC effective precipitation model

This was carried out by comparing raster maps of the CIHAM-UC-EP with the US-SCS-EP models (Farias *et al.* 2020a).

## Calibration of forecasting models for components of CIHAM-UC-EP model

The stage of forecasting of CIHAM-UC-EP implies two sequential steps: (a) fitting of forecasting models for

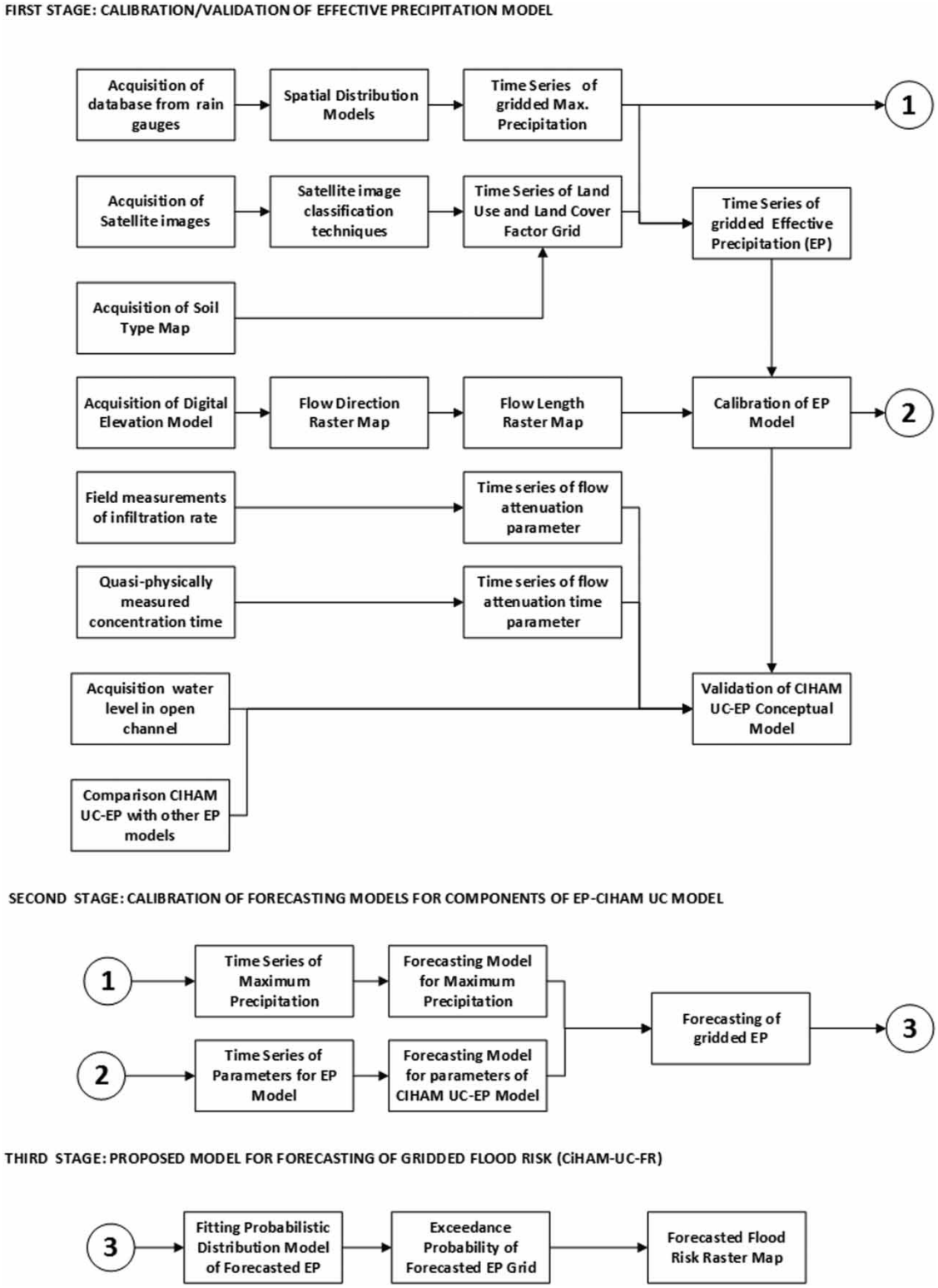


**Figure 2** | Scheme of proposed method for forecasting flood risk by CIHAM-UC.

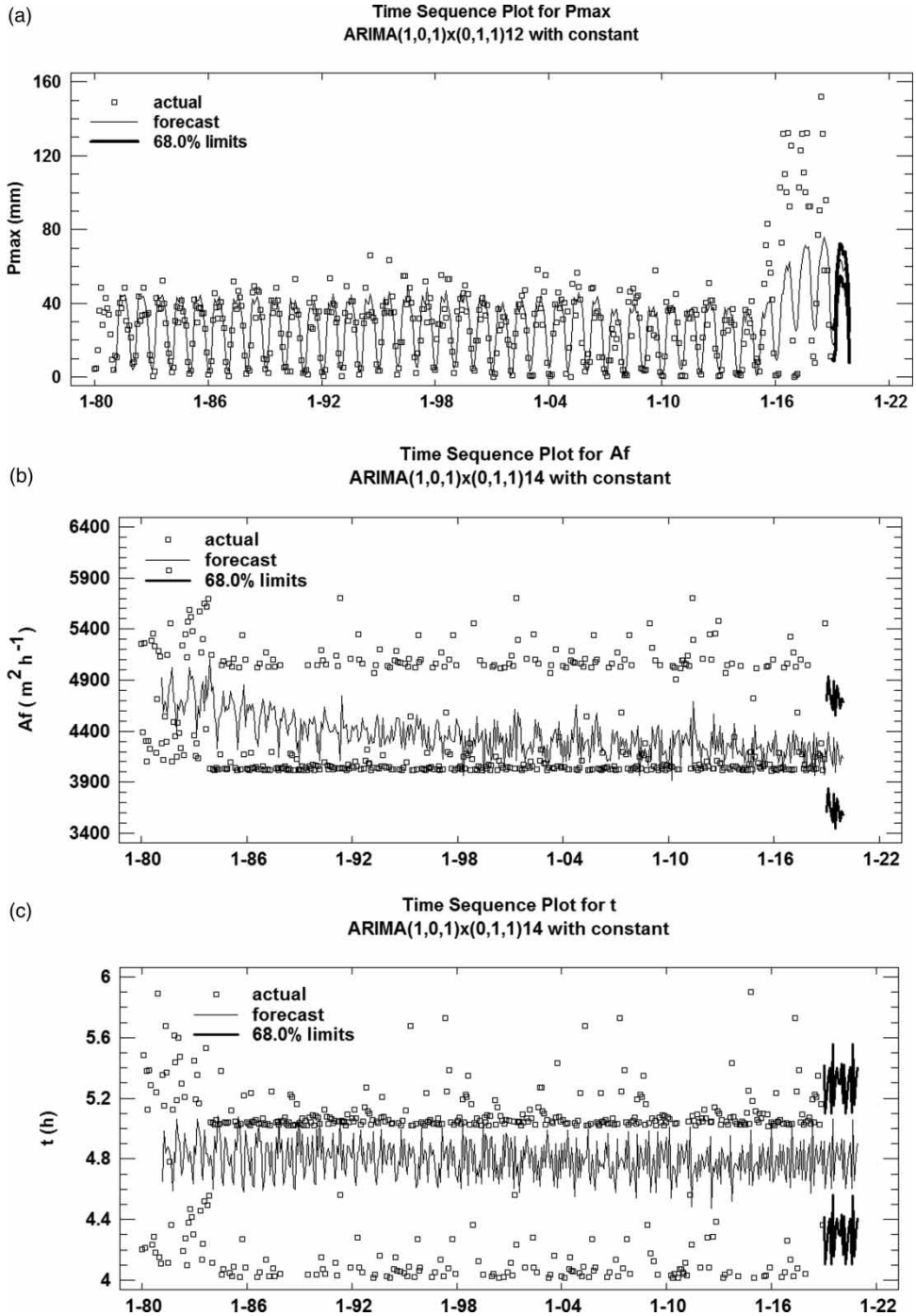


**Figure 3** | Time series models of components for forecasting of effective precipitation: (a) maximum precipitation for duration of six hours, (b) parameter $A_f$, (c) parameter $t$.

components of CIHAM-UC-EP and (b) forecasting of the components of CIHAM-UC-EP for future events.

(a) **Fitting of forecasting models for components of CIHAM-UC-EP (Figure 3):** five ARIMA models are evaluated for mathematical fitting to the components of the CIHAM-UC-EP model ($P_{max}$, $A_f$, $t$) extracted from the processing of 456 maps for the period 1980–2018. The forecasting models for the components of the

CIHAM-UC-EP model are chosen by comparing the results of applying the statistical errors.

(b) **Forecasting of the components of CIHAM-UC-EP for future events (Figure 3):** the forecasting models are applied to obtain the results for a future date. The forecast components are substituted in the CIHAM-UC-EP model to predict the forecast raster map of CIHAM-UC-EP.

## Proposed model for forecasting of gridded flood risk (CIHAM-UC-FR)

The generation of the forecast flood risk map involves two steps (Figure 2): (a) fitting of a probabilistic distribution model of the forecast CIHAM-UC-EP, (b) determining of the exceedance probability of the forecasted CIHAM-UC-EP grid and (c) generation of the forecast flood risk map:

(a) **Fitting of probabilistic distribution model of forecast CIHAM-UC-EP:** 13 probabilistic distribution models were tested for adjusting to the CIHAM-UC-EP selecting exponential function, and the best fitting to the forecasted CIHAM-UC-EP was log likelihood.

(b) **Determining of exceedance probability of forecast CIHAM-UC-EP grid:** the curve of exceedance probability of the forecast CIHAM-UC-EP dataset was obtained from statistical software. The raster map of exceedance probability of the forecast CIHAM-UC-EP was produced by applying a conversion function from the polygon layer in GIS.

(c) **Proposed model for forecasting of gridded flood risk (CIHAM-UC-FR):** the generation of the forecast flood risk map was carried out by applying Equation (11) used as a unique input to the raster map of exceedance probability of forecast CIHAM-UC-EP setting four values to the parameter $n$ from 1 to 100 (Figure 4).

# RESULTS AND DISCUSSION

The results of applying the method for the forecasting of the spatial distribution of flood risk in the study area are presented according to three stages (Figure 2): (1) calibration and validation of the effective precipitation model, (2) forecasting of effective precipitation and (3) estimating of the spatial distribution of forecast flood risk.

## Results of the calibration and validation of effective precipitation model

### Analysis of monthly time series of maximum precipitation for an event duration of 6 h

The trend cycle (TC) is estimated by smoothing the $P_{max}$ time series data represented by the continuous trace (Figure 3(a)), using a moving average, which is distanced by observed data in a difference equal to the seasonality varying between 4 and 15 during the period 1980–2018.

### Analysis of monthly time series of flow attenuation parameter for an event duration of 6 h

The midpoint in the trend cycle is at 4,150 $m^2\,h^{-1}$ (Figure 3(b)), and the flow attenuation parameter ($A_f$) is associated with the infiltration process in natural channels and terrain. The rate of infiltration can be estimated from parameter $A_f$ assuming that the absorption of flow along the flow length occurs in areas with natural coverage such as forests and degraded soil. In the study area, the flow length varies between 1,586 and 3,984 m, with the result that the infiltration rate varies from 2.6 $m\,h^{-1}$ to 1 $m\,h^{-1}$ (2,610 to 1,000 $mm\,h^{-1}$).

Tests of infiltration rate were made taking measures in time intervals from 2 and 137 minutes ranging in values less than 400 $mm\,h^{-1}$ for a cumulative probability of 75%, and atypical values between 600 and 2,400 $mm\,h^{-1}$ (Márquez 2009; Márquez & Guevara 2011a; Guevara & Márquez 2012). By comparing, the field measurements of infiltration rate with the values found evaluating the magnitude of coefficient $A_f$ for a determined flow length, similar results have been found.

### Analysis of monthly time series of flow attenuation time parameter for precipitation event duration of 6 h

The quasi-physically measured concentration time is estimated by comparing values by applying Manning's

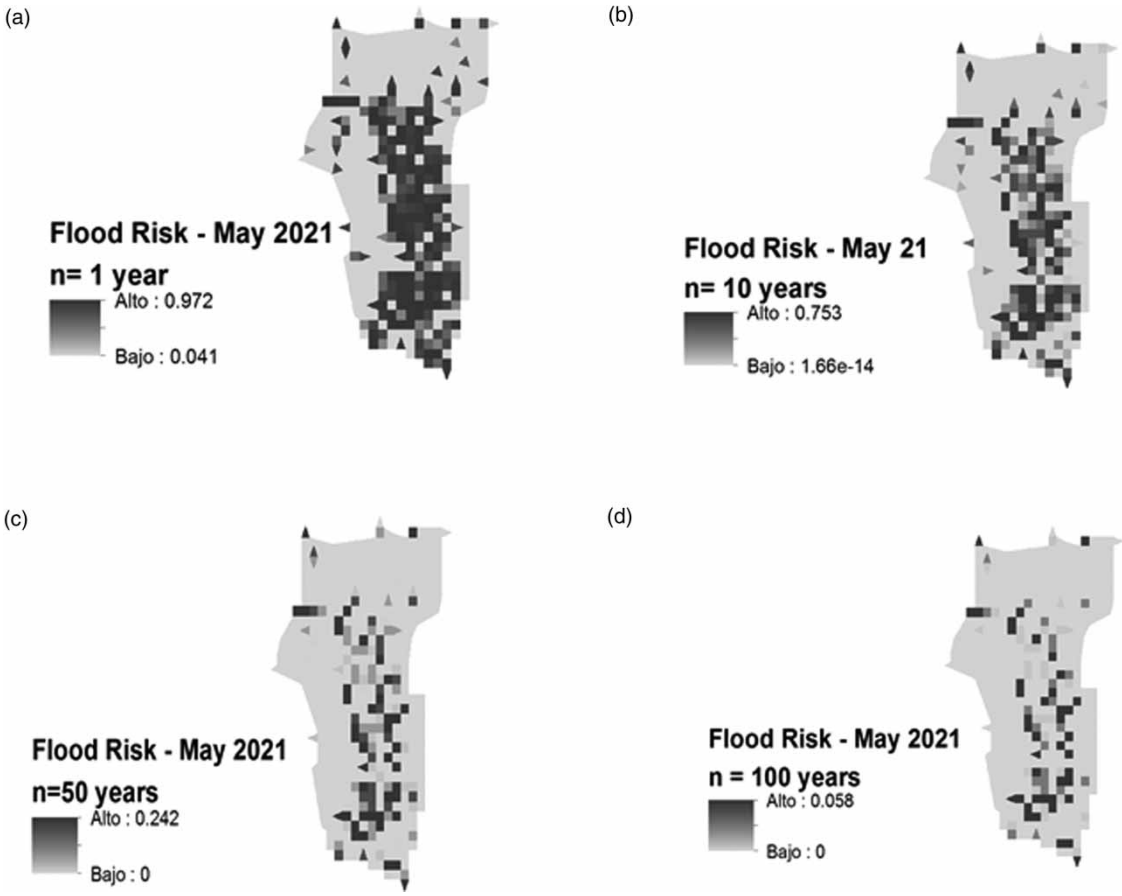


**Figure 4** | Scenarios for flood risk forecast for May 2021 in the study area, the Cabriales River basin, Venezuela, according to the useful life of hydraulics works: (a) $n = 1$ year, (b) $n = 10$ years, (c) $n = 50$ years, (d) $n = 100$ years.

equation referred to as one of the main components of concentration time using GIS commands (Feldman 2000). The estimated velocities through Manning's equation range between 1 and 7 m $s^{-1}$ for a cumulative frequency of 79%. Therefore, the channel travel times resulting ranged between 1.5 and 7 h. The values meaning a fraction of concentration time are a reference that represent an order of 1:1.5 greater than the trend cycle of the flow attenuation time (Figure 3(c)). The flow attenuation time should run in the initial stage of precipitation event occurrence in natural areas of the watershed because of the descent trend of the exponential pattern associated with the infiltration rate process, explained as due to the aerated spaces in the soil matrix and the water saturation subsequent of micro-conduits after an elapsed time greater than one hour.

### Validation of CIHAM-UC effective precipitation model comparing results of CIHAM-UC-EP model with other models

The results of the US-SCS-EP model found by Farias *et al.* (2020a) give a spatial distribution where EP has a small deviation between the maximum and minimum values because of the equation structure being a ratio based on water balance, overestimating EP by comparing with the spatial distribution obtained by applying the CIHAM-UC-EP-model on the same study area.

## Calibration of forecasting models for components of CIHAM-UC-EP model

The calibration and validation stages of the forecasting models for $P_{max}$ and parameters $A_f$ and $t$ give as a result

an ARIMA model (1, 0, 1)$x$(0, 1, 1)$s$ (Table 1). In this model structure, the nonseasonal autoregressive term is of order 1 (AR(1)), the nonseasonal differencing of is order 0, the nonseasonal moving average term is of order 1 (MA(1)), the seasonal autoregressive term is of order 0, the seasonal differencing is of order 1, and the seasonal moving average term is of order 1 (SMA(1)). The selected model has one order of total differencing, resulting in the following expression (Box & Jenkins 1970):

$$\hat{Y}_t = \mu + Y_{t-s} + \phi_1(Y_{t-1} - Y_{t-s}) + e_t - \theta_1 e_{t-1} - \Theta_1 e_{t-s} + \theta_1\Theta_1 e_{t-s} \quad (12)$$

where $\phi_1$ is the AR(1) parameter, $\theta_1$ is the MA(1) parameter and $\Theta_1$ is the SMA(1) parameter. In the three fittings of the ARIMA model (Table 1), two time series are used as input data corresponding to the periods 1980–2000 and 1980–2018. The values of the SMA(1) coefficient near 1.0 are due to between ten and 20 seasons of data being used to calculate the historical average for given months from 20 to 38 years (Table 1). The seasonality ($s$) is of 12 months for the $P_{max}$ time series and 14 months for the $A_f$ and $t$ parameters.

The errors in the time series of $P_{max}$, $A_f$ and $t$ in the period 1980–2000 are similar for the calibration and validation stages, indicating that the model passes five statistical tests related to excessive runs up and down, above and below median, autocorrelation, difference in mean and variance. The influence of residual autocorrelations is non-significant due to the model describing all of the dynamic structure in a time series.

For the $P_{max}$ time series during the period 1980–2018, there is high variance in values measured during the period 2015–2018 (Figure 3(a)), which explains the difference between errors in the calibration and validation stages (Table 1). The influence of the AR(1) and MA(1) coefficients on the independent variable for the time series 1980–2000 is lower in the order of two times than those values for the time series 1980–2000. The future prediction predominantly reproduces the observed pattern in $P_{max}$ during the period 1980–2015.

The prediction intervals of mean values for $P_{max}$, $A_f$ and $t$ in the period 1980–2000 are made based on the 68% confidence level that includes a standard deviation from the mean value, which represents the upper and lower limits shown in Figure 3, where it can be seen that the prediction is close to the forecast mean value.

## Proposed model for forecasting of gridded flood risk (CIHAM-UC-FR)

### Fitting probabilistic distribution model of forecast EP

By applying the log likelihood statistic to nine probabilistic distribution functions (PDF), the following orders of

**Table 1** | Fitted parameters and statistical errors of ARIMA models to variables and parameters of flood risk method

| | | | | ARIMA model parameters | | | | | Statistical errors | | | | |
|---|---|---|---|---|---|---|---|---|---|---|---|---|---|
| Period | Variable | Stage | N° | AR(1) | MA(1) | SMA(1) | Constant | s | RMSE | MAE | MAPE | ME | MPE |
| 1980–2018 | $P_{max}$ | C | 468 | − 0.25 | − 0.30 | 0.88 | 0.23 | 12 | 7.65 | 5.39 | 65.7 | −0.02 | −48.5 |
| | | V | 234 | | | | | | 22.8 | 13.6 | 242.1 | 3.3 | −217.0 |
| | $A_f$ | C | 468 | 0.61 | 0.50 | 0.91 | − 9.12 | 14 | 533.4 | 471.3 | 10.41 | −38.9 | −2.12 |
| | | V | 234 | | | | | | 537.2 | 412.7 | 8.74 | 153.7 | 2.34 |
| | $t$ | C | 468 | 0.07 | 0.05 | 0.91 | − 0.0008 | 14 | 0.4 | 0.4 | 8.73 | −0.001 | −1.02 |
| | | V | 234 | | | | | | 0.48 | 0.4 | 9.29 | 0.005 | −0.9 |
| 1980–2000 | $P_{max}$ | C | 240 | − 0.41 | − 0.57 | 0.81 | − 0.07 | 12 | 5.3 | 4.1 | 53.13 | 0.02 | −36.6 |
| | | V | 120 | | | | | | 9.4 | 6.7 | 67.31 | 1.34 | −41.5 |
| | $A_f$ | C | 252 | 0.44 | 0.28 | 0.86 | − 42.22 | 14 | 546.5 | 473.0 | 10.45 | −67.3 | −2.7 |
| | | V | 126 | | | | | | 595.0 | 416.3 | 8.63 | 279.1 | 5.2 |
| | $t$ | C | 252 | 0.06 | − 0.002 | 0.84 | − 0.003 | 14 | 0.49 | 0.40 | 8.65 | 0.01 | −0.7 |
| | | V | 126 | | | | | | 0.48 | 0.41 | 9.15 | −0.001 | −1.1 |

AR(1), non-seasonal autoregressive term; MA(1), non-seasonal moving average term; SMA, seasonal moving average term; $s$, seasonality; C, calibration; V, validation; RMSE, root mean squared error; MAE, mean absolute error; MAPE, mean absolute percentage error; ME, mean error; MPE, mean percentage error.

magnitude are found: (1) Exponential, Largest Extreme Value ($-5\times10^4$), (2) Normal, Logistic, Smallest Extreme Value ($-6\times10^4$), (3) Lognormal, Weibull, Gamma, Log-logistic ($-1\times10^9$). The best effective precipitation fit to PDF is the exponential function. The fitted model for the exceedance probability is represented by a decreasing exponential equation, whose parameters are a coefficient $a$ (0.99) and exponent $b$ (0.042) as follows:

$$P(X \geq x) = ae^{-b(EP)} = 0.99e^{-0.042(EP)} \quad (13)$$

### Exceedance probability of forecast EP grid

The exceedance probability of the forecast CIHAM-UC-EP grid shows that the highest exceedance probability varying between 56% and 96%, occurs where the natural coverage is mostly distributed (forested area, degraded soil). The lowest exceedance probability is found in the urban area (25%–56%).

### Proposed model for forecasting of gridded flood risk

The proposed equation for forecasting of flood risk can be expressed by substituting the equation associated with the exceedance probability in Equation (11).

The scenarios obtained from application of the CIHAM-UC-FR model (Equation (11)), for forecast flood risk during May 2021 in a watershed within the Pao River basin, Cabriales River basin, Venezuela, are shown in Figure 4, varying the expected life of hydraulic structures for 1, 10, 50 and 100 years. The flood risk is permanently low in the mountainous area, close to zero, and takes values near to 1 in the urban area. The flood risk is decreased as the expected life of hydraulic structures is increased based on a power function, and by substituting Equation (13) in Equation (11), the resulting expression is as follows:

$$FR = [1 - ae^{-b(EP)}]^n = [1 - 0.99e^{-0.042(EP)}]^n \quad (14)$$

where the fitted parameters are $a$ and $b$, and the effective precipitation is obtained by the CIHAM-UC-EP model.

## CONCLUSIONS

A novel method for forecasting gridded flood risk has been created from the Center of Hydrological and Environmental Research of the University of Carabobo (CIHAM-UC, in Spanish) called CIHAM-UC-FFR, obtaining appropriate results for water management in vulnerable areas to flooding events such as the urban fraction of land use and land cover (LULC) in a study area at a watershed scale, because of the occurrence of the rainfall–runoff process. The main purpose of the CIHAM-UC-FFR method is to provide information to make decisions for contributing to the prevention of the consequences of flooding by protecting human beings and goods.

The proposed method might be classified as a hybrid, which can be applied for obtaining lumped or distributed values in the forecast main variables of interest, estimated using models proposed for the effective precipitation (CIHAM-UC-EP) and flood risk (CIHAM-UC-FR) depending on availability of local information. In general, the CIHAM-UC-FFR method includes various model categories for its components: (1) CIHAM-UC-EP (event, conceptual/quasi-conceptual, lumped/distributed, measured/fitted parameters), (2) precipitation (event, distributed/lumped, empirical, stochastic, fitted parameter), (3) parameters of CIHAM-UC EP (event, lumped, empirical, stochastic, fitted parameter), (4) probabilistic function for CIHAM-UC EP (event, lumped/distributed, empirical, stochastic, fitted parameter), (5) CIHAM-UC-FR (event, distributed, empirical, deterministic, fitted parameter).

The advantages of applying the proposed method are based on the following. (1) The update of the calibration of the equations due to it offering an easy incorporation of new information for making continuous recalibration of the components for the CIHAM-UC-EP model by using time series of precipitation measured from rain gauges and time series of satellite images for the LULC factor. (2) The adaptability of the three parameters included in the CIHAM-UC-EP model to be derived using algorithms for mathematical adjustment or obtained from field measurements, which means that CIHAM-UC-EP can be classified as a conceptual or quasi-conceptual model. The flow attenuation parameter ($A_f$) might be obtained measuring infiltration rate for a determined flow length, expressed in

$m^2\ h^{-1}$. The flow attenuation time ($t$) can be obtained from the quasi-physically measured concentration time. (3) The capability of the model to explain the temporal variation of flow depth ($\partial h/\partial t$) depending on the terrain elevations, flow path and the flow length in the terrain establishing a strong difference with other models, whose results tend to be homogeneous in watersheds. (4) The capability to adapt the components of the CIHAM-UC-EP model to multiple forecasting models for time series. (5) The perspective of change in the response obtained from the CIHAM-UC-FR model supported on the exceedance probability of the EP and its association with the flood risk process, being adapted to various scenarios in periods from short (monthly) to long term (annually) according to the increase of expected life of the hydraulic structure.

It is recommended for future evaluations of the CIHAM-UC-EP and CIHAM-UC-FR models to increase the spatio-temporal resolution of the involved parameters and variables and to compare with field measurements to validate the obtained results.

## REFERENCES


Box, G. E. P. & Jenkins, G. M. 1970 *Time Series Analysis: Forecasting and Control*. Holden-Day, San Francisco, CA, USA.

Chow, V. T., Maidment, D. R. & Mays, L. W. 1988 *Applied Hydrology: International Edition*. MacGraw-Hill Inc., New York, USA.

Farias, B., Márquez, A., Rey, D. & Guevara, E. 2018 Characterization spatio-temporal land use in watershed using geomatic techniques. *Revista Ingenieria UC* **25** (1), 19–30. http://servicio.bc.uc.edu.ve/ingenieria/revista/v25n1/vol25n12018.pdf

Farias, B., Marquez, A., Guevara, E. & Rey, D. 2020a Plan de gestión sustentable de riesgo de inundación: una propuesta desde la Universidad de Carabobo (Sustainable flood risk management plan: a proposal from the University of Carabobo). *REDER Revista de Estudios Latinoamericanos sobre Reducción del Riesgo de Desastres*. **4** (1), 67–79. https://mailchi.mp/db1f48982a50/vol4-num1

Farias, B., Marquez, A., Guevara, E. & Rey, D. 2020b Method for flood risk estimation in a tropical basin. *Water Supply* **20** (2), 712–723. doi:10.2166/ws.2019.202.

Feldman, A. D. 2000 *Hydrologic Modeling System HEC-HMS: Technical Reference Manual*. US Army Corps of Engineers, Hydrologic Engineering Center, Davis, CA, USA. https://www.hec.usace.army.mil/software/hec-hms/documentation/HEC-HMS_Technical%20Reference%20Manual_(CPD-74B).pdf

Fleming, M. J. & Doan, J. H. 2013 *HEC-GeoHMS Geospatial Hydrologic Modeling Extension: User's Manual*. US Army Corps of Engineers, Davis, CA, USA. https://www.hec.usace.army.mil/software/hec-geohms/documentation/HEC-GeoHMS_Users_Manual_4.2.pdf

Guevara, E. 2016 Transporte y transformación de contaminantes en el ambiente y contaminación de las aguas (Transport and transformation of pollutants in the environment and water pollution). Ministerio de Agricultura y Riego, Lima, Perú. https://hdl.handle.net/20.500.12543/3941

Guevara, E. & Cartaya, H. 2004 *Hidrología Ambiental*. Facultad de Ingeniería de la Universidad de Carabobo, Valencia, Venezuela.

Guevara, E. & Márquez, A. M. 2012 Modeling of the infiltration in a crop field of Chirgua basin, Carabobo state, Venezuela. *Revista Científica UDO Agrícola* **12** (2), 365–388.

Infante, S., Ortega, J. & Cedeño, F. 2008 Estimación de datos faltantes en estaciones meteorológicas de Venezuela vía un modelo de redes neuronales (Estimation of missing data in Venezuelan meteorological stations via a neural network model). *Revista de Climatología* **8**, 51–70. https://s3.amazonaws.com/academia.edu.documents/46961810/

Márquez, A. M. 2009 *Hydrologic Modeling with Applications in Geographic Information Systems*. Delforn Editions, Venezuela.

Márquez, A. M. & Guevara, E. 2011a Modeling of erosion and sediment transport in furrows in a farm field under irrigation in Venezuela. *Tecnología y Ciencias del Agua* **2** (2), 125–156 http://www.scielo.org.mx/scielo.php?script=sci_arttext&pid=S2007-24222011000200009

Márquez, A. M. & Guevara, E. 2011b Estimating infiltration parameters based on soil physical properties of agricultural land in Venezuela. *Revista Ingeniería UC* **18** (1), 65–79. http://servicio.bc.uc.edu.ve/ingenieria/revista/V18n1/art08.pdf

Márquez, A. M. & Guevara, E. 2013 Rainfall runoff model calibration for floodplain zoning in Unare River basin, Venezuela. In: *35th IARH World Congress*, Chengdu, China. https://www.tib.eu/en/search/id/BLCP%3ACN086216199/Rainfall-Runoff-Model-Calibration-for-the-Floodplain/

Márquez, A. M. & Guevara, E. 2016 Forecasting of the input, turbined and output flows of the Simon Bolivar hydroelectric power plant, Venezuela. In: *XXVII Latin American Congress of Hydraulics*, Lima, Peru, September 2016. http://www.apiha.org/blog/libro-resumenes-extendidos-xxvii-congreso-latinoamericano-hidraulica-lima-2016, http://www.mediafire.com/file/bey3nxgap3tp83w/LIBRO_RESUMENES_EXTENDIDOS-LADHI2016-APIHA_%2528ultimo%2529.pdf/file

Márquez, A. M., Guevara, E. & Rey, D. 2018 Assessment of land use and land cover change detection using eleven techniques of satellite remote sensing in the Pao River Basin, Venezuela. *Journal of Remote Sensing GIS & Technology* **4** (2). http://matjournals.in/index.php/JORSGT/article/view/2764

Márquez, A. M., Guevara, E. & Rey, D. 2019 Hybrid model for forecasting of changes in land use and land cover using satellite techniques. *IEEE Journal of Selected Topics in Applied Earth Observations and Remote Sensing* **12** (1), 252–273. https://ieeexplore.ieee.org/abstract/document/8605374/

Meza, E. 2007 *Propuesta de diseño de un sistema de comunicaciones alterno para la interconexión del sistema de radares meteorológicos a la sede del INAMEH (Proposal for the Design of an Alternate Communication System for the Interconnection of the Meteorological Radar System to the INAMEH Headquarters)*. Tesis de Grado, Universidad Central de Venezuela, Caracas, Venezuela. http://saber.ucv.ve/bitstream/123456789/770/1/TrabajodegradoErika.pdf

Olivera, F., Maidment, D. R. & Reed, S. 1998 HEC-PrePro v. 2.0: An ArcView pre-processor for HEC's hydrologic modeling system. In: *Proceedings of the 18th ESRI Users Conference, San Diego, CA, USA*, July, pp. 25–31. https://proceedings.esri.com/library/userconf/proc98/proceed/TO400/PAP400/P400.HTM

Schumann, A. H. (ed.) 2011 *Flood Risk Assessment and Management: How to Specify Hydrological Loads, Their Consequences and Uncertainties*. Springer Science & Business Media, Dordrecht, The Netherlands.

Sene, K. 2008 *Flood Warning, Forecasting and Emergency Response*. Springer Science & Business Media, Berlin, Germany.

Soil Conservation Service 1986 *Urban Hydrology for Small Watersheds*. Technical Release 55, USDA, Springfield, VA, USA.

Szymkiewicz, R. 2010 *Numerical Modeling in Open Channel Hydraulics*. Springer Science & Business Media, Dordrecht, The Netherlands.

First received 19 February 2020; accepted in revised form 8 June 2020. Available online 18 June 2020